NASA TECHNICAL NOTE

NASA TN D-3979

NASA TN D-3979

FREQUENCY RESPONSE AND TRANSFER FUNCTIONS OF A NUCLEAR ROCKET ENGINE SYSTEM OBTAINED FROM ANALOG COMPUTER SIMULATION

by Clint E. Hart and Dale J. Arpasi

Lewis Research Center
Cleveland, Ohio

NATIONAL AERONAUTICS AND SPACE ADMINISTRATION • WASHINGTON, D. C. • MAY 1967

NASA TN D-3979

FREQUENCY RESPONSE AND TRANSFER FUNCTIONS OF A NUCLEAR ROCKET ENGINE SYSTEM OBTAINED FROM ANALOG COMPUTER SIMULATION

By Clint E. Hart and Dale J. Arpasi

Lewis Research Center
Cleveland, Ohio

NATIONAL AERONAUTICS AND SPACE ADMINISTRATION

For sale by the Clearinghouse for Federal Scientific and Technical Information
Springfield, Virginia 22151 – CFSTI price $3.00

FREQUENCY RESPONSE AND TRANSFER FUNCTIONS OF A NUCLEAR ROCKET ENGINE SYSTEM OBTAINED FROM ANALOG COMPUTER SIMULATION

by Clint E. Hart and Dale J. Arpasi

Lewis Research Center

SUMMARY

The dynamic response characteristics of the basic variables of a NERVA-type nuclear rocket engine system are presented. Frequency-response data, at four selected operating levels, were obtained from a detailed analog computer simulation. Frequency responses of thrust chamber temperature, chamber pressure, and reactor power to pertinent control or system variables are shown.

Transfer functions that approximate the frequency responses are presented. The effect of reactor period on the reactor-power transfer function was investigated, and transfer functions are presented for 2.0 and 0.5 seconds, as well as for infinite periods. These results provide essential information for control system analysis and design.

The analytical models and assumptions used to develop the equations that represent the dynamics of nuclear rocket engine components are discussed. A set of specific equations that can be used in an analog computer simulation is presented.

INTRODUCTION

Extensive experimental testing is being conducted in the NERVA program to provide data for the design of a nuclear rocket engine system. Although the type of engine system under consideration was found to operate stably without closed-loop control, transient operational requirements necessitate the use of a closed-loop control system. These requirements include rapid startup (possibly 60 to 90 sec from flow initiation to full thrust), precise control of thrust and specific impulse, and controlled shutdown and restart.

For the design of such a control system, either transfer functions or frequency responses of some basic engine system variables to other system or control variables are required. During the experimental tests conducted thus far, two methods were used to

obtain these frequency responses or transfer functions. These methods were (1) direct measurement of the frequency responses to sinusoidal input signals and (2) measurement of responses to random noise input signals and use of cross-correlation data processing techniques (ref. 1).

Neither method yielded sufficient frequency-response data or transfer-function information to complete a comprehensive control-system design. The main reasons for the scarcity of this information are the difficulty of obtaining measured signals with good signal-to-noise ratios and the limited amount of running time allotted to this type of test.

System transfer functions can be analytically derived from the set of algebraic and nonlinear differential equations that describe the system behavior (refs. 2 and 3). However, this is a formidable task. Many simplifying assumptions are required to derive reasonable transfer functions. The validity of these assumptions has not been thoroughly investigated.

A fourth method is to simulate the nuclear rocket engine system by programing an analog computer to solve a set of system equations and to obtain the required frequency-response data from this simulation.

The purposes of this study were (1) to obtain frequency responses of basic engine system variables to other system or control variables at several steady-state operating levels and (2) to determine the approximate transfer functions that represent these frequency responses.

A set of equations was developed that represents the principal dynamic characteristics of a nuclear rocket engine system over a range from approximately 20 to 120 percent of the design conditions of thrust chamber pressure and temperature. A nonlinear, wide-range analog computer simulation was programed from this set of equations; frequency responses of reactor power, thrust chamber pressure and temperature were obtained at four selected operating levels.

Approximate transfer functions that represent these frequency responses were determined. In addition, reactor-power transfer functions that are dependent on reactor period were developed. These transfer functions are essential for control system design by root-locus techniques.

SYSTEM CONFIGURATION

The nuclear rocket engine system considered in this study is shown schematically in figure 1. The pump receives the liquid hydrogen, that is stored at low pressure in the propellant tank and delivers it at high pressure through a discharge line to the inlet of the nozzle coolant tubes. The hydrogen vaporizes in the nozzle coolant tubes. Then the hydrogen vapor flows through the reflector, shield, and reactor core passages and is ex-

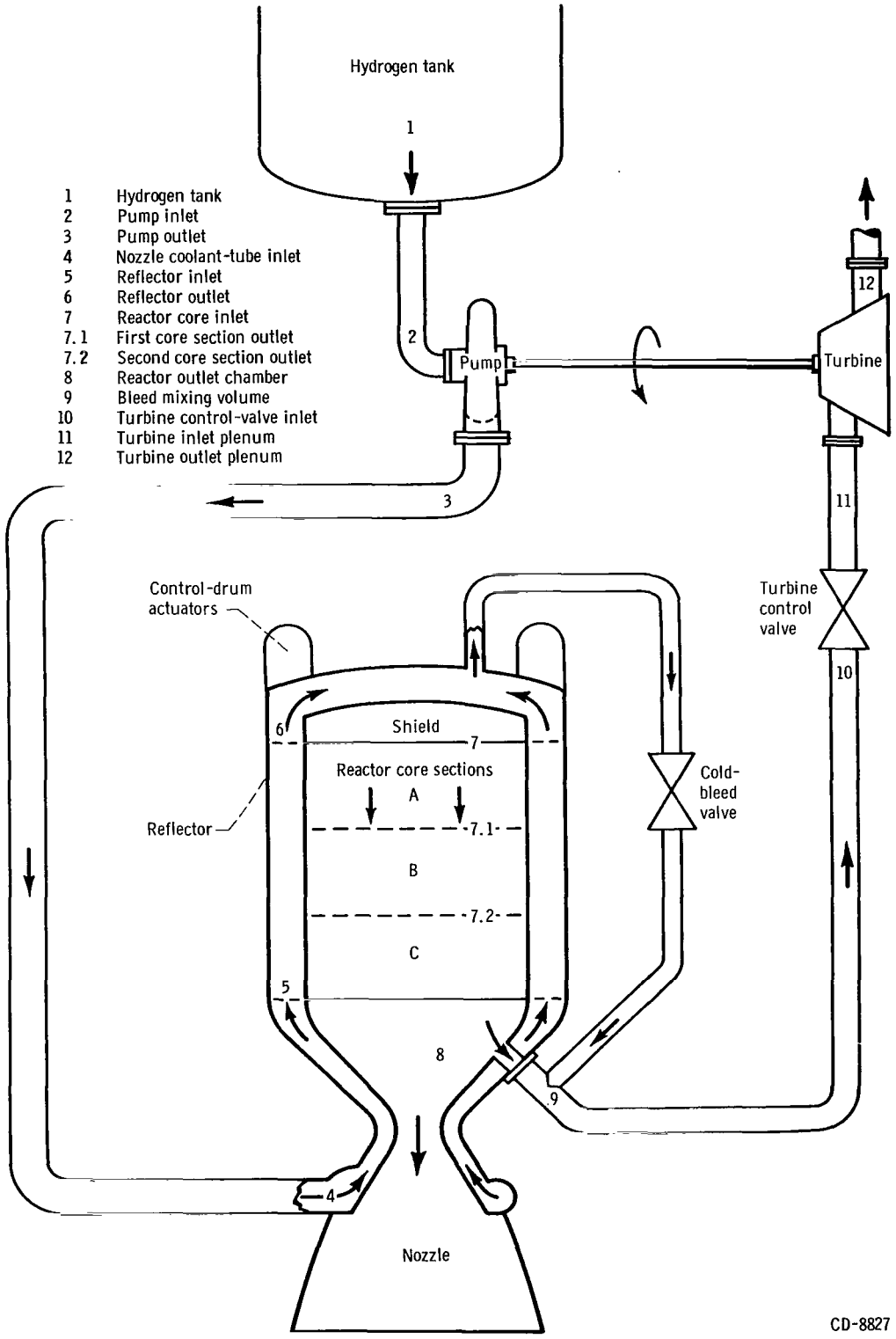

Figure 1. - Schematic drawing of nuclear rocket engine.

pelled at high velocity through the nozzle to provide thrust. Heat is transferred, principally by convection, to the hydrogen as it flows through the system.

The hot-bleed cycle provides the turbine hot-gas source. Gas of the proper temperature to drive the turbine is obtained by controlled mixing of hot gas tapped from the reactor outlet chamber and cold gas from the reactor inlet plenum. Turbine weight flow, and hence torque, is controlled by a valve in the bleed line.

The reactor is a solid-core thermal type with highly enriched uranium fuel and a graphite moderator. The reflector is a beryllium sleeve surrounding the core. Cylindrical control drums, with neutron poison plates covering part of their surface, are rotated to control reactor power. These control drums are located in the reflector.

SYSTEM EQUATIONS AND ASSUMPTIONS

The equations that describe the dynamic behavior and interrelation of the engine system variables consist of a set of ordinary and partial differential equations and some algebraic equations. To develop a set of equations for analog computer simulation of a system, the geometric complexities of the system must be reduced and a simpler, analytical model formulated. Furthermore, the partial differential equations must be reduced to ordinary differential equations since the analog computer normally performs operations with respect to only one independent variable. Finite-difference techniques were used to reduce the equations to time-dependent differential equations.

In the following paragraphs of this section, the analytical models and assumptions for the various components comprising a nuclear rocket engine system are discussed and the general equations that evolve from these models are given. The specific equations used in the analog computer simulation are given in appendix B. These equations are based on the design data for a first-generation NERVA-type nuclear rocket engine that develops approximately 56 000 pounds of thrust. The station designations used in the specific equations are shown in figure 1.

Reactor Core

The analytical model assumed for developing the reactor-core heat-transfer equations is a cylinder with a single flow passage divided axially into three equal-length sections. The following discussion applies to one section.

Taking a heat balance on the material and assuming the average wall temperature to be equal to the average material temperature yielded the following equation:

$$\frac{dq_m}{dt} = \dot{Q}_m - hA_s\left(\bar{T}_m - \frac{T_{in} + T_{out}}{2}\right) \tag{1}$$

(All symbols are defined in appendix A.) The first term on the right side represents the thermal power generated in the section, and the second term represents the heat transferred by convection to the propellant. The heat content of the core section was obtained by integrating equation (1).

The average material temperature $\bar{T}_m$ is considered to be a function of the heat content q_m. Since the specific heat of the core material varies considerably with temperature, the heat content is defined as the mass times the integrated specific heat of the material, and is in equation form

$$q_m = \rho_m V_m \int_0^{\bar{T}_m} c_m \, d\bar{T}_m \tag{2}$$

The heat-transfer coefficient h in equation (1) was determined by using the following correlation equation from reference 4

$$\frac{hD}{k} = 0.025\, Re^{0.8} Pr^{0.4}\left(\frac{T_w}{T_b}\right)^{-0.55}\left[1 + 0.3\left(\frac{L}{D}\right)^{-0.7}\right] \tag{3}$$

with k, Re, and Pr evaluated at bulk conditions. The L/D correction was negligible for the analytical models considered in this study.

The following heat balance equation was obtained for the propellant contained within the flow passage:

$$\frac{dq_H}{dt} = hA_s\left(\bar{T}_m - \frac{T_{in} + T_{out}}{2}\right) - \dot{W}(H_{out} - H_{in}) \tag{4}$$

In the system under study, the thermal time constant of the propellant is of the order of 1 millisecond, while the thermal time constant of the core material is of the order of 1 second. Thus, in the frequency range of interest (up to 100 rad/sec), the thermal dynamics in the propellant can be neglected. Equation (4) then can be reduced to

$$hA_s\left(\bar{T}_m - \frac{T_{in} + T_{out}}{2}\right) = \dot{W}(H_{out} - H_{in}) \tag{5}$$

The enthalpy of the propellant at the core inlet is considered to be a function of pressure and temperature at temperatures below 240° R, but only a function of temperature at temperatures at or above 240° R. The enthalpy of the propellant at other locations in the core is considered to be only a function of temperature.

The momentum or pressure-drop equation used in this study is

$$P_{in} - P_{out} = \frac{L}{144g}\left(\frac{\dot{W}}{A}\right)^2\left[v_{out} - v_{in} + \frac{4fL}{D}\left(\frac{1}{\bar{\rho}}\right)\right] + \frac{L}{144gA}\frac{d\dot{W}}{dt} \tag{6}$$

Over the range of conditions encountered in the flow passages, the term $1/\bar{\rho}$ can be approximated by $(v_{in} + v_{out})/4$. Inlet and outlet specific volumes were computed from pressures and temperatures by use of the state equation for a perfect gas. Additional pressure losses at the inlet and exit of the flow passage were also considered.

When the momentum equation (eq. (6)) was applied to the reactor core, the dynamic contribution of the last term was assumed to be negligible, and the equation was solved for weight flow rate. As a compromise between accuracy and the analog components required, only one axial section was assumed for the reactor core when equation (6) was used. The friction factor was assumed to be constant in the reactor core.

Reactor Kinetics

The reactor-kinetics equations were used in this study in the standard linear form as follows:

$$\frac{dn}{dt} = \frac{\delta K}{l^*}n - \frac{\beta}{l^*}n + \sum_{i=1}^{6}\lambda_i C_i \tag{7}$$

$$\frac{dC_i}{dt} = \frac{\beta_i}{l^*}n - \lambda_i C_i \tag{8}$$

The values of the decay constants and the relative abundance of the six delayed-neutron groups were obtained from reference 5.

Reactivity

The total reactivity increases or decreases reactor power according to the reactor-kinetics equations. Total reactivity consists of the inherent reactivity feedback plus the

reactivity due to the control drums. The inherent reactivity feedback is a rather complicated phenomenon, which, for the purposes of this study, was assumed to consist of the reactivity related to material temperature changes in the core and to hydrogen density changes in the core flow passages.

The inherent reactivity feedback is given by the equation

$$\delta K_I = F(\overline{T}_{mc}, \overline{\rho}_H) \tag{9}$$

The average material temperature in the core $\overline{T}_{mc}$ is approximated by the linear average of the material temperatures in the three axial sections. The density of the hydrogen in the core changes over a wide range from inlet to outlet and is not linear with core length. Thus, the average hydrogen density $\overline{\rho}_H$ cannot be determined by simple averaging techniques. For the range of variables encountered in this study, the following equation is a good approximation of the average hydrogen density in the core:

$$\overline{\rho}_H = \frac{144 P_{in}}{R(T_{out} - T_{in})} \ln \frac{T_{out}}{T_{in}} \tag{10}$$

Pump

The pump inlet pressure and temperature were assumed to be constant and equal to tank conditions. The pump pressure rise and torque were determined from functional relations among pressure rise, torque, weight flow rate, and speed. Typical pump maps, which were obtained from experimental data by plotting pressure rise against weight flow rate for constant speeds and constant efficiencies, were converted to single-curve functional relations defined by the following equations:

$$\frac{P_{out} - P_{in}}{N^2} = F_1\left(\frac{\dot{W}_p}{N}\right) \tag{11}$$

$$\frac{M_p}{N^2} = F_2\left(\frac{\dot{W}_p}{N}\right) \tag{12}$$

Density was assumed to be constant throughout the pump. The temperature rise between the pump inlet and outlet was assumed to be proportional to weight flow for this study.

Pump Discharge Line

The momentum equation (eq. (6)) was solved for $d\dot{W}/dt$ and integrated to obtain pump weight flow rate. The specific volume and the friction factor were assumed to be constant, and the temperature rise in the discharge line was assumed to be zero.

Nozzle

The analytical model assumed for the nozzle coolant passages was a single tube with one axial section. Although the tube geometry was quite complex, equivalent constant-area tube properties were used in the pressure-drop and heat-transfer equations. The momentum equation (eq. (6)) was solved for the inlet pressure; the $d\dot{W}/dt$ term was neglected. Inlet specific volume and friction factor were assumed to be constant. Outlet specific volume was determined from outlet pressure and temperature by using the state equation.

Nuclear heat generation in the nozzle wall material and thermal radiation to the nozzle walls from the hot core were assumed to be negligible. Thus, a heat-balance equation for the nozzle wall material can be written as

$$\frac{dq_m}{dt} = h_{hg}A_s(\overline{T}_{hg} - \overline{T}_m) - h_{nc}A_s\left(\overline{T}_m - \frac{T_{in} + T_{out}}{2}\right) \tag{13}$$

The first term on the right side represents the heat transferred from the hot gas to the nozzle wall material, and the second term represents the heat transferred from the material to the hydrogen flowing through the coolant tubes. In this study the nozzle heat-transfer coefficients are assumed to vary only with weight flow to the 0.8 power. Equation (13) was integrated to obtain the heat content of the wall material. As in the core, the material temperature was considered to be a function of the heat content.

The nozzle coolant outlet enthalpy and temperature were obtained by solving equation (5) for outlet enthalpy and considering outlet temperature as a function of enthalpy and pressure.

Reflector

Although the reflector contains different materials and also flow passages of various sizes and shapes, it is not feasible in this system-dynamics study to solve equations representing the heat transfer and fluid flow of all the different types of flow passages in

parallel. Instead, a single cylinder and flow passage with one axial section was assumed for the reflector model. The size of the flow passage was determined from total flow area and heat-transfer surface area. The physical and thermal properties of the cylinder material were based on weighted averages of the properties of aluminum, beryllium, and graphite.

The thermal dynamics in the reflector are represented by equations (1) to (3) and (5) with the proper coefficients. Equation (5) was solved for coolant outlet temperature. The enthalpy of the hydrogen at the reflector inlet was considered to be a function of both temperature and pressure because, in this study, the temperature at this point was always below 240° R. The reflector pressure drop is represented by the momentum equation (eq. (6)). However, this equation was solved for the inlet pressure and the $\dot{W}$ term was neglected.

Reactor-Core Inlet Plenum and Shield

The density of the hydrogen in the core inlet plenum was obtained by integrating the following continuity equation:

$$V \frac{d\rho}{dt} = \sum \dot{W} \tag{14}$$

The pressure in the plenum was computed by using the state equation and assuming uniform density and temperature throughout the plenum. The heat transfer and pressure drop in the shield were considered to be negligible for this study.

Thrust Chamber and Nozzle

The continuity equation (eq. (14)) and the state equation were used to determine the density and pressure of the hydrogen in the thrust chamber. For this study, the thrust nozzle was assumed to be choked at all times and nozzle weight flow rate was computed from the equation

$$\dot{W} = K \frac{P}{T^{0.5}} \tag{15}$$

Bleed System and Turbine Control Valve

A portion of the turbine bleed line was considered to be a mixing volume. The density and pressure in the mixing volume were computed by using the continuity equation (eq. (14)) and the state equation. The hot bleed gas was considered to flow through a fixed orifice and the cold bleed gas through a valve in the cold bleed line.

The cold-bleed, hot-bleed, and valve weight flow rates were computed by using the following compressible-flow equation:

$$\dot{W} = A \frac{P}{T^{0.5}} \left[\frac{2g}{R} \left(\frac{\gamma}{\gamma - 1} \right) \right]^{0.5} (PR)^{1/\gamma} \left[1 - (PR)^{(\gamma-1)/\gamma} \right]^{0.5} \tag{16}$$

In this equation, P and T are values upstream of the orifice or valve, and PR is the ratio of downstream to upstream pressures. The turbine control valve is a butterfly-type valve. The effective flow area is a function of the shaft angular position of the valve.

Since the cold-bleed, hot-bleed, and valve weight flow rates were at different temperatures, a form of energy-balance equation was used to compute the heat content of the hydrogen in the mixing volume. The enthalpy of the hydrogen in the mixing volume was computed by integrating the following equation:

$$\rho V \frac{dH}{dt} = \dot{W}_{hb} H_{hb} + \dot{W}_{cb} H_{cb} - \dot{W}_{v} H \tag{17}$$

Then, from an enthalpy-temperature relation, the average temperature in the mixing volume was obtained. To apply this equation in this study, the dynamics associated with mass storage were assumed to be negligible.

Turbine and Turbopump Dynamics

The section of line from the turbine control valve to the turbine inlet was considered the turbine inlet plenum. The turbine inlet temperature was assumed to be equal to the temperature in the bleed mixing volume. The continuity equation (eq. (14)) and the state equation were used to determine the density and pressure in the turbine inlet plenum.

The turbine weight flow rate was computed from the following equation:

$$\dot{W}_t = \frac{P_{ti}}{T_t^{0.5}} F\left(\frac{p_{te}}{P_{ti}} \right) \tag{18}$$

For pressure ratios less than 0.3, the functional relation is essentially constant. The turbine torque was computed by using the following equation:

$$M_t = \dot{W}_t \left\{ K_1 T_{ti}^{0.5} \left[1 - \left(\frac{p_{te}}{P_{ti}} \right)^{\gamma - 1/\gamma} \right]^{0.5} - K_2 N \right\} \tag{19}$$

The pressure ratio used in equations (18) and (19) is the ratio of turbine-exit static pressure to turbine-inlet total pressure.

An outlet plenum and exhaust nozzle were assumed to be downstream of the turbine. The density in the outlet plenum was determined by integrating the continuity equation (eq. (14)). The weight flow rate through the exhaust nozzle was computed by using the compressible-flow equation (eq. (16)) with appropriate constants.

The enthalpy drop across the turbine was determined from the power output of the turbine (i.e., the product of torque and speed). Then, if specific heat is assumed to be constant, the following equation for turbine exit temperature can be derived:

$$T_{te} = T_t - \frac{M_t N \pi}{30 \dot{W}_t c_p J} \tag{20}$$

In this study, the static temperature computed by this equation was assumed to be equal to the total temperature.

The total pressure in the turbine outlet plenum was computed by using the state equation. The static pressure can be determined by subtracting $\rho u^2/2g$ from the total pressure. The resulting equation for turbine-exit static pressure is

$$p_{te} = P_{te} - \frac{R T_{te} \dot{W}_t^2}{2 g p_{te} A^2} \tag{21}$$

The turbopump speed was obtained by integrating the following torque-balance equation:

$$\frac{dN}{dt} = \frac{30}{\pi I} (M_t - M_p) \tag{22}$$

COMPUTER SIMULATION OF SYSTEM

Analog Computer Simulation

The system equations listed in appendix B were programed and set up on two 100-amplifier analog computer consoles. The complement of computer components required consisted of 190 amplifiers, 70 multipliers, and 20 diode-function generators. The time scale was 1 to 1 (i.e., real time). Amplitude scaling permitted the simulation to cover the following ranges of the primary variables: temperature, 50° to 5000° R; pressure, 10 to 1000 pounds per square inch absolute; weight flow rate, 5 to 100 pounds per second; and reactor power, 20 to 2000 megawatts.

Digital Computer Solution of Steady-State Equations

Amplitude scaling a large analog simulation to operate over a wide range of the system variables is a difficult problem. Optimum scaling at one operating point may cause scaling problems at other points. Knowledge of the steady-state values of the system variables at many operating points is required to scale the analog simulation properly for maximum accuracy over a wide operating range. Therefore, the steady-state system equations were programed for digital computer solution.

The steady-state values obtained from the digital computer program were used not only to assist in scaling the analog simulation but also to check the validity of the analog setup and the overall accuracy of the analog simulation.

One way to present the results of the steady-state calculations is shown in figure 2.

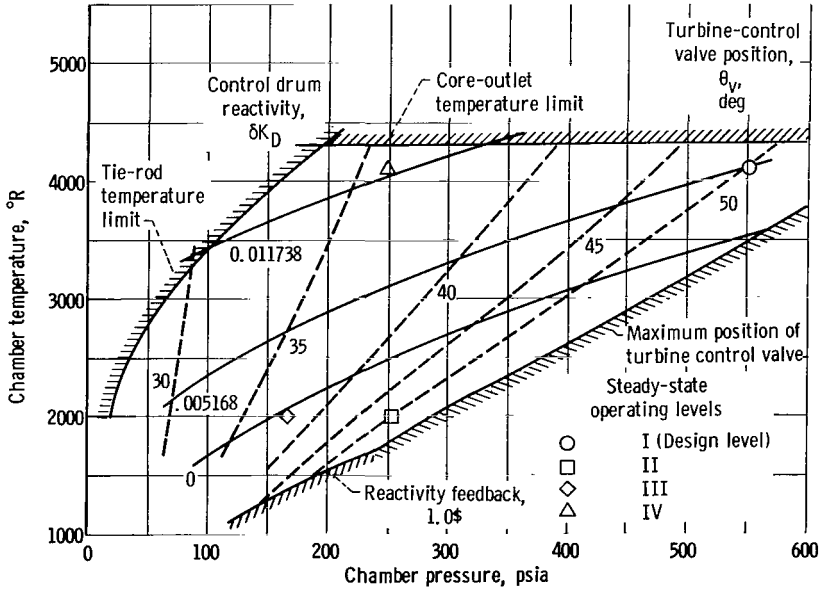

Figure 2. - Map of steady-state operating conditions with constraints.

Lines of constant control-drum reactivity and constant turbine-control-valve position are plotted as functions of chamber temperature and pressure. The boundaries or constraints on the allowable operating region are imposed by system component limitations or operational requirements. The sensitivities of engine system variables to changes in the input variables can be estimated from this figure, but more complete information regarding system dynamics is presented and discussed in the following sections.

FREQUENCY RESPONSE AND TRANSFER FUNCTIONS

An analog computer simulation such as the one described herein can be used to obtain the frequency response of the engine system variables to changes in the input variables. This information is needed by the control-system designer to select feedback control-loop configurations and controller compensations properly, and to specify dynamic performance requirements of the control-loop hardware.

One control concept that has evolved from various studies is, basically, to control reactor outlet-chamber temperature by manipulating the control drums and reactor outlet-chamber pressure by manipulating a turbine control valve. Figure 3 is a block diagram of this control concept. In addition to the primary control loops, a reactor-power control loop is used as an inner loop to the chamber temperature loop. In this control concept, the primary frequency-response data pertinent to control-system design include

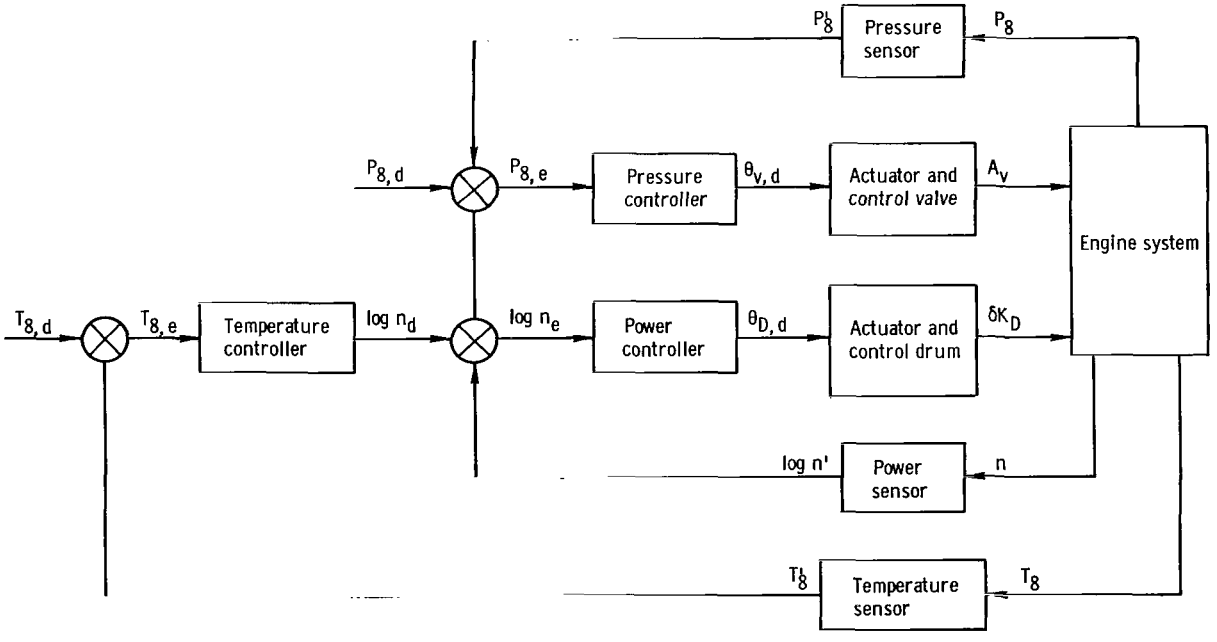

Figure 3. - Block diagram of control system for nuclear rocket engine.

(1) Response of chamber temperature to reactor power, $\Delta T_8/\Delta \dot{Q}$

(2) Response of chamber pressure to turbine-control-valve position, $\Delta P_8/\Delta \theta_v$

(3) Response of reactor power to control-drum reactivity, $\Delta n/\Delta \delta K_D$

The control system may be required to provide stable operation over a wide range of the system variables. Therefore, frequency-response data were obtained from the analog computer simulation at design level and three other operating levels. The four operating levels are shown in figure 2. The steady-state values of reactor power, core weight flow, chamber pressure and temperature are tabulated in table I.

TABLE I. - STEADY-STATE VALUES OF SYSTEM VARIABLES

Steady-state operating level	Thermal power generated ($\propto$n), $\dot{Q}$, Btu/sec	Reactor outlet chamber temperature, T_8, ^{o}R	Reactor outlet chamber total pressure, P_8, psi	Reactor weight flow rate, $\dot{W}_c$, lb/sec
I	1.067×10^{6}	4090	550	72.15
II	3.252×10^{5}	2000	253	48.03
III	2.122	2000	167	31.43
IV	4.780	4090	250	32.41

Frequency-response data can be used directly to determine graphically, by means of Bode plots and Nichols charts, the open-loop and closed-loop frequency response of the system with various feedback control-loop configurations and controller compensations. Another graphical analysis technique that can be used is the root-locus technique. This technique generally is faster and provides more insight into the effects of the controller on the transient response of a system. However, to apply the root-locus technique, it is necessary to have the system dynamic response in transfer-function form.

Equipment and Procedure

A frequency-response analyzer was used to obtain the frequency-response data. This equipment consists of a variable-frequency sinusoidal oscillator and a signal analyzer. The analyzer calculates the amplitude ratio and phase shift between an input and output signal of the component or system being tested or simulated.

With the analog computer simulation operating at a steady-state level, a sinusoidal signal from the oscillator was added to one of the input variables. The resulting response of the selected output variable was fed to the signal analyzer, which calculated and dis-

played an amplitude-ratio and a phase-shift reading. The amplitude-ratio reading was corrected to account for amplitude scaling of the analog computer signals. This procedure was repeated for other input signal frequencies over the range of interest and also for various combinations of input and output variables.

An Electro Scientific Industries Algebraic Computer (ESIAC) was used to determine transfer functions that approximate the frequency-response data. This special type of analog computer and some of its applications are described in references 6 and 7. For this application, the poles and zeros of the trial transfer function were adjusted until the

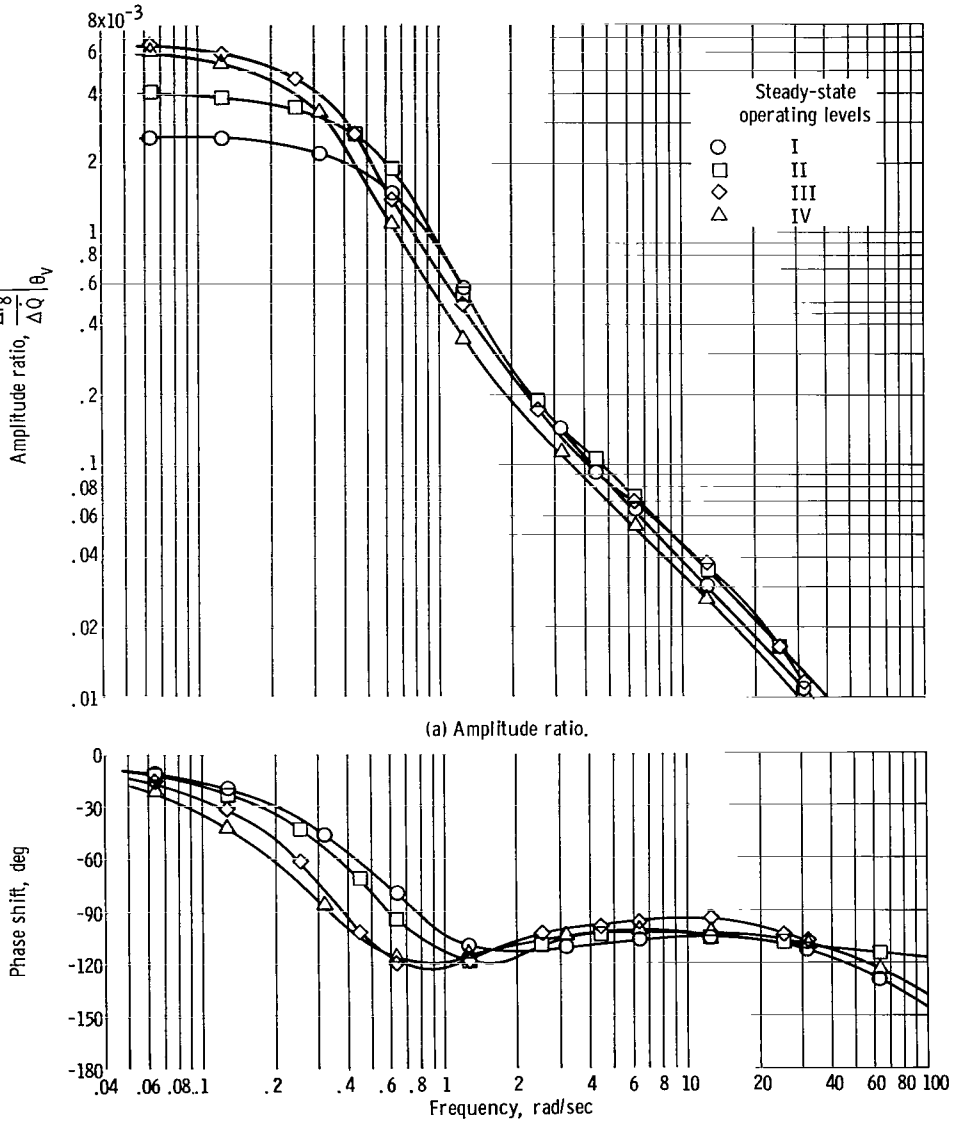

Figure 4. - Frequency response of reactor-outlet-chamber temperature to reactor power, obtained from analog computer simulation. Turbine-control-valve position held constant at each steady-state operating level.

frequency response calculated by the ESIAC computer matched the analog frequency-response data to the desired accuracy. An agreement of $\pm 5^{\circ}$ in phase shift and ±10 percent in amplitude was considered satisfactory.

Response of Chamber Temperature to Reactor Power

The frequency response of chamber temperature to reactor power at four steady-state operating levels is shown in figure 4. Data for these curves were obtained from the analog computer simulation with the turbine-control-valve position held constant at each level.

The transfer functions that approximate these frequency-response curves are listed in table II. No attempt was made to derive these transfer functions from the system equations. The steady-state gain terms indicate an inverse relation to core weight flow. Attempts to correlate the time constants with any of the system variables were unsuccessful.

TABLE II. - TRANSFER FUNCTIONS OF CHAMBER TEMPERATURE TO REACTOR POWER

Steady-state operating level	Transfer function, $\left[\Delta T_8(s)/\Delta \dot{Q}(s)\right]_{\theta_v}$
I	$\dfrac{2.6\times10^{-3}\left(1+\dfrac{s}{1.55}\right)}{\left[1+\dfrac{1.4\,s}{0.5}+\left(\dfrac{s}{0.5}\right)^2\right]\left(1+\dfrac{s}{90}\right)}$
II	$\dfrac{3.67\times10^{-3}\left(1+\dfrac{s}{1.55}\right)}{\left[1+\dfrac{1.4\,s}{0.45}+\left(\dfrac{s}{0.45}\right)^2\right]\left(1+\dfrac{s}{90}\right)}$
III	$\dfrac{6.75\times10^{-3}\left(1+\dfrac{s}{1.25}\right)}{\left[1+\dfrac{1.4\,s}{0.27}+\left(\dfrac{s}{0.27}\right)^2\right]\left(1+\dfrac{s}{90}\right)}$
IV	$\dfrac{6.0\times10^{-3}\left(1+\dfrac{s}{1.2}\right)}{\left[1+\dfrac{1.4\,s}{0.26}+\left(\dfrac{s}{0.26}\right)^2\right]\left(1+\dfrac{s}{90}\right)}$

Response of Chamber Pressure to Turbine-Control-Valve Position

The frequency response of chamber pressure to turbine-control-valve position at the four steady-state operating levels is shown in figure 5. These data were obtained with constant control-drum position at each level. Approximating transfer functions for these frequency-response curves are listed in table III.

Response of Reactor Power to Control-Drum Reactivity

The frequency response of reactor power to control-drum reactivity at the four steady-state operating levels is

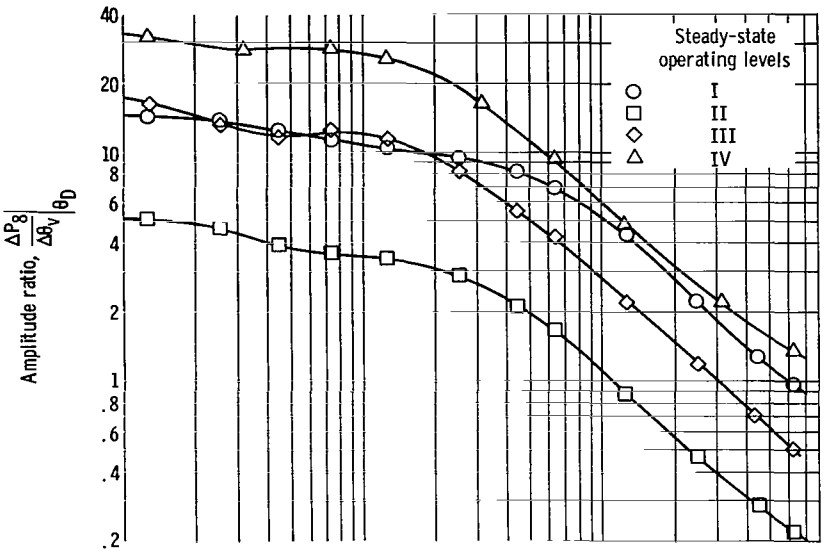

(a) Amplitude ratio.

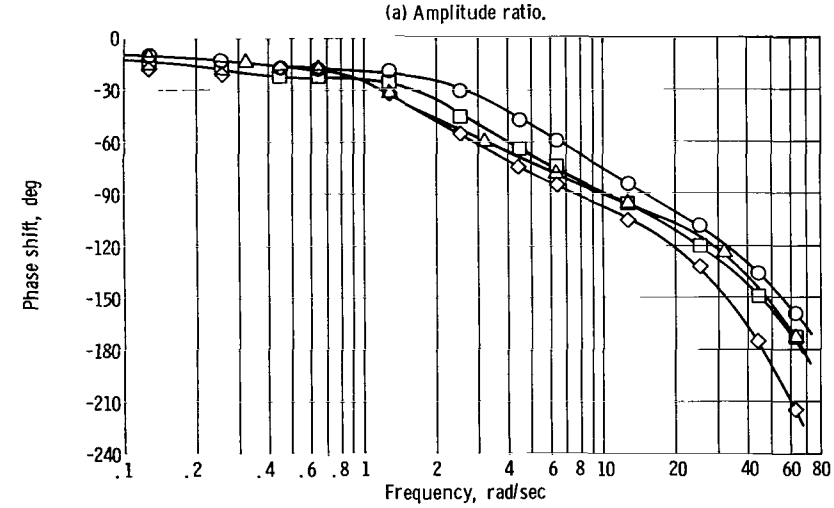

(b) Phase shift.

Figure 5. - Frequency response of reactor-outlet-chamber pressure to turbine-control-valve position, obtained from analog computer simulation. Control-drum position held constant at each steady-state operating level.

TABLE III. - TRANSFER FUNCTIONS OF CHAMBER PRESSURE TO TURBINE-CONTROL-VALVE POSITION

Steady-state operating level	Transfer function, $\left[\Delta P_8(s)/\Delta\theta_V(s)\right]_{\theta_D}$
I	$\frac{16.5\left(1+\frac{s}{0.45}\right)e^{-0.020\,s}}{\left(1+\frac{s}{0.29}\right)\left(1+\frac{s}{5.3}\right)}$
II	$\frac{5.95\left(1+\frac{s}{0.30}\right)e^{-0.024\,s}}{\left(1+\frac{s}{0.18}\right)\left(1+\frac{s}{3.2}\right)}$
III	$\frac{20.0\left(1+\frac{s}{0.145}\right)e^{-0.035\,s}}{\left(1+\frac{s}{0.09}\right)\left(1+\frac{s}{2.5}\right)}$
IV	$\frac{35.0\left(1+\frac{s}{0.17}\right)e^{-0.022\,s}}{\left(1+\frac{s}{0.14}\right)\left(1+\frac{s}{2.3}\right)}$

shown in figure 6. Data for these curves were obtained with the turbine-control-valve position held constant at each level.

Designing reactor control systems requires a reactor transfer function different from the one normally obtained for steady-state power operation. Control systems designed by considering the steady-state reactor transfer function have exhibited unexpected oscillations during rapid power increases. Investigation of this phenomenon led to the explanation of the "period equilibrium effect" in reactor dynamics and the derivation of a reactor kinetics transfer function that is dependent on reactor period (ref. 8).

The data for the frequency-response curves shown in figure 6 were obtained by perturbing the system at steady-state power levels. Thus, the curves represent essentially the response at infinite reactor period. The frequency response at finite-equilibrium periods is not readily obtainable from the analog computer simulation. Thus, another approach was used to obtain period-dependent reactor transfer functions. This approach is based upon the relation among the reactor kinetics, the inherent reactivity feedback, and the desired reactor transfer function $\Delta\dot{Q}/\Delta\delta K_D$, as shown in the block diagram in figure 7.

In appendix C, a transfer function that represents period-dependent reactor kinetics is discussed. Also presented in this appendix are specific transfer functions calculated for the system design values of ℓ^* and β, and for infinite, 2- and 0.5-second periods.

The transfer functions of inherent reactivity feedback to reactor power for the four steady-state operating levels are listed in table IV. These transfer functions were determined by approximating the frequency response obtained from the analog computer simulation.

The transfer functions listed in table IV were combined with the corresponding reactor-kinetics transfer functions for each operating level to obtain the desired closed-loop transfer functions $\Delta\dot{Q}/\Delta\delta K_D$. The ESIAC computer was used to find the roots of the equations that represent the denominators of the closed-loop transfer functions. The closed-loop transfer functions thus obtained are listed in table V.

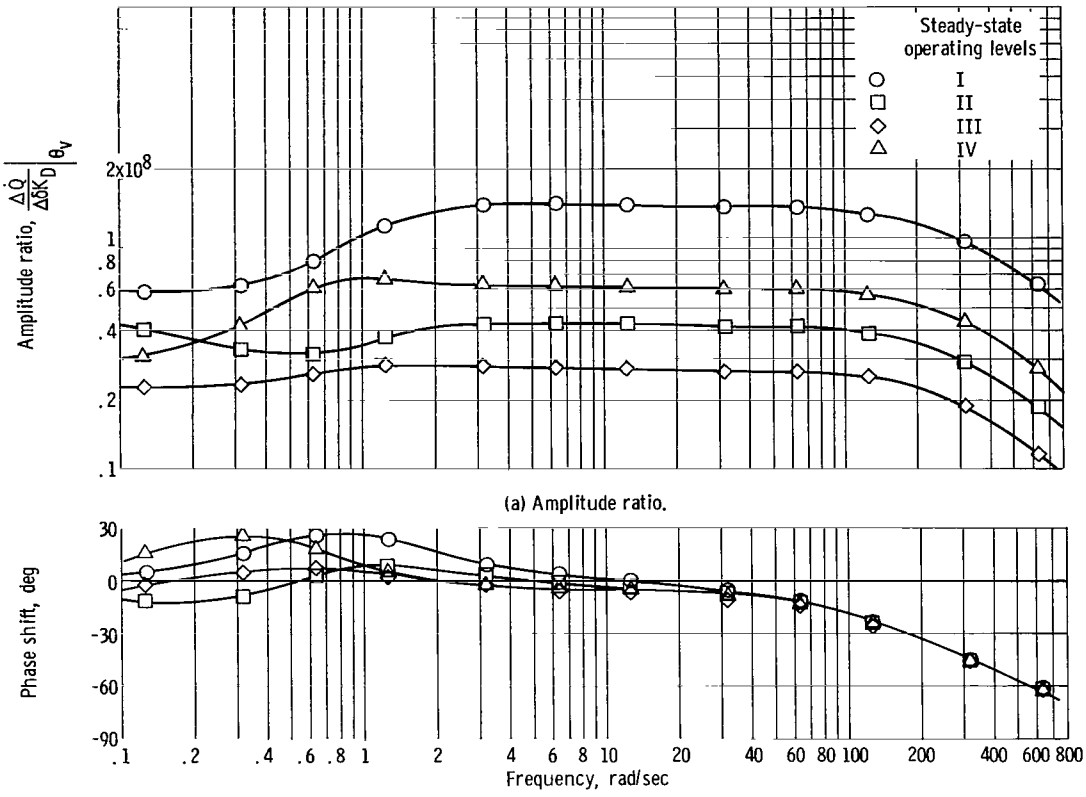

Figure 6. - Frequency response of reactor power to control-drum reactivity, obtained from analog computer simulation. Turbine-control-valve position held constant at each steady-state operating level.

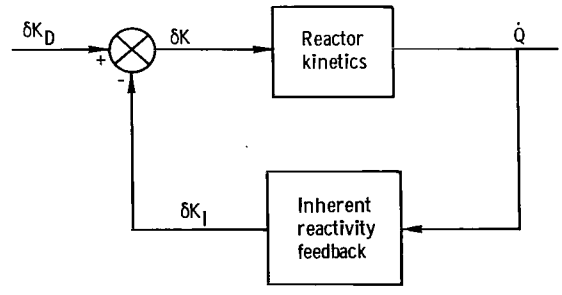

Figure 7. - Block diagram of reactivity loop.

TABLE IV. - TRANSFER FUNCTIONS OF INHERENT REACTIVITY FEEDBACK TO REACTOR POWER

Steady-state operating level	Transfer function, $\left[\Delta\delta K_I(s)/\Delta\dot{Q}(s)\right]_{\theta_v}$
I	$\frac{1.4\times10^{-8}}{\left(1+\frac{s}{0.48}\right)\left(1+\frac{s}{71}\right)}$
II	$\frac{2.1\times10^{-8}}{\left(1+\frac{s}{0.7}\right)\left(1+\frac{s}{68}\right)^2}$
III	$\frac{3.4\times10^{-8}}{\left(1+\frac{s}{0.4}\right)\left(1+\frac{s}{73}\right)^2}$
IV	$\frac{3.27\times10^{-8}}{\left(1+\frac{s}{0.2}\right)\left(1+\frac{s}{90}\right)}$

The effect of reactor period on the reactor-power dynamic response is shown in figure 8. In this figure are the frequency-response curves that represent the three period-dependent transfer functions for operating level I listed in table V. Also plotted in figure 8 are frequency-response data obtained from the analog computer simulation at operating level I. The agreement between analog data and the infinite period curve is reasonably good.

TABLE V. - TRANSFER FUNCTIONS OF REACTOR POWER TO CONTROL-DRUM REACTIVITY

Steady-state operating level	Reactor period, sec	Transfer function, $\left[\Delta\dot{Q}(s)/\Delta\delta K_D(s)\right]_{\theta_v}$
I	Infinite	$\dfrac{7.14\times10^7\left(1+\frac{s}{0.0276}\right)\left(1+\frac{s}{0.235}\right)\left(1+\frac{s}{0.48}\right)\left(1+\frac{s}{1.65}\right)}{\left(1+\frac{s}{0.0241}\right)\left(1+\frac{s}{0.204}\right)\left[1+\frac{1.85\,s}{1.45}+\left(\frac{s}{1.45}\right)^2\right]\left(1+\frac{s}{312}\right)}$
	2	$\dfrac{7.14\times10^7\left(1+\frac{s}{0.48}\right)\left(1+\frac{s}{0.735}\right)\left(1+\frac{s}{2.15}\right)\left(1+\frac{s}{71}\right)}{\left(1+\frac{s}{0.82}\right)\left[1+\frac{1.68\,s}{2.45}+\left(\frac{s}{2.45}\right)^2\right]\left(1+\frac{s}{62}\right)\left(1+\frac{s}{102}\right)}$
	0.5	$\dfrac{7.14\times10^7\left(1+\frac{s}{0.48}\right)\left(1+\frac{s}{2.24}\right)\left(1+\frac{s}{3.65}\right)\left(1+\frac{s}{71}\right)}{\left(1+\frac{s}{2.53}\right)\left[1+\frac{1.51\,s}{4.7}+\left(\frac{s}{4.7}\right)^2\right]\left(1+\frac{s}{30}\right)\left(1+\frac{s}{81}\right)}$
II	Infinite	$\dfrac{4.76\times10^7\left(1+\frac{s}{0.0276}\right)\left(1+\frac{s}{0.235}\right)\left(1+\frac{s}{0.7}\right)\left(1+\frac{s}{1.65}\right)}{\left(1+\frac{s}{0.0208}\right)\left(1+\frac{s}{0.17}\right)\left[1+\frac{1.88\,s}{1.4}+\left(\frac{s}{1.4}\right)^2\right]\left(1+\frac{s}{312}\right)}$
	2	$\dfrac{4.76\times10^7\left(1+\frac{s}{0.7}\right)\left(1+\frac{s}{2.15}\right)\left(1+\frac{s}{68}\right)^2}{\left[1+\frac{1.83\,s}{2.1}+\left(\frac{s}{2.1}\right)^2\right]\left(1+\frac{s}{51}\right)\left(1+\frac{s}{83}\right)\left(1+\frac{s}{102}\right)}$
	0.5	$\dfrac{4.76\times10^7\left(1+\frac{s}{0.7}\right)\left(1+\frac{s}{2.24}\right)\left(1+\frac{s}{3.65}\right)\left(1+\frac{s}{68}\right)^2}{\left(1+\frac{s}{2.58}\right)\left[1+\frac{1.34\,s}{4}+\left(\frac{s}{4}\right)^2\right]\left(1+\frac{s}{25.5}\right)\left[1+\frac{1.93\,s}{79}+\left(\frac{s}{79}\right)^2\right]}$
III	Infinite	$\dfrac{2.94\times10^7\left(1+\frac{s}{0.0276}\right)\left(1+\frac{s}{0.235}\right)\left(1+\frac{s}{0.4}\right)\left(1+\frac{s}{1.65}\right)}{\left(1+\frac{s}{0.0212}\right)\left(1+\frac{s}{0.184}\right)\left(1+\frac{s}{0.82}\right)\left(1+\frac{s}{1.24}\right)\left(1+\frac{s}{312}\right)}$
	2	$\dfrac{2.94\times10^7\left(1+\frac{s}{0.4}\right)\left(1+\frac{s}{0.735}\right)\left(1+\frac{s}{2.15}\right)\left(1+\frac{s}{73}\right)^2}{\left(1+\frac{s}{1.05}\right)\left[1+\frac{1.51\,s}{1.35}+\left(\frac{s}{1.35}\right)^2\right]\left(1+\frac{s}{55}\right)\left(1+\frac{s}{84}\right)\left(1+\frac{s}{102}\right)}$
	0.5	$\dfrac{2.94\times10^7\left(1+\frac{s}{0.4}\right)\left(1+\frac{s}{2.24}\right)\left(1+\frac{s}{3.65}\right)\left(1+\frac{s}{73}\right)^2}{\left(1+\frac{s}{2.55}\right)\left[1+\frac{1.0\,s}{2.9}+\left(\frac{s}{2.9}\right)^2\right]\left(1+\frac{s}{34}\right)\left[1+\frac{1.96\,s}{79}+\left(\frac{s}{79}\right)^2\right]}$
IV	Infinite	$\dfrac{3.06\times10^7\left(1+\frac{s}{0.0276}\right)\left(1+\frac{s}{0.2}\right)\left(1+\frac{s}{0.235}\right)\left(1+\frac{s}{1.65}\right)}{\left(1+\frac{s}{0.0246}\right)\left(1+\frac{s}{0.255}\right)\left(1+\frac{s}{0.535}\right)\left(1+\frac{s}{1.28}\right)\left(1+\frac{s}{312}\right)}$
	2	$\dfrac{3.06\times10^7\left(1+\frac{s}{0.2}\right)\left(1+\frac{s}{0.735}\right)\left(1+\frac{s}{2.15}\right)}{\left(1+\frac{s}{1.15}\right)\left[1+\frac{1.41\,s}{1.33}+\left(\frac{s}{1.33}\right)^2\right]\left(1+\frac{s}{102}\right)}$
	0.5	$\dfrac{3.06\times10^7\left(1+\frac{s}{0.2}\right)\left(1+\frac{s}{2.24}\right)\left(1+\frac{s}{3.65}\right)}{\left(1+\frac{s}{2.76}\right)\left[1+\frac{1.0\,s}{3}+\left(\frac{s}{3}\right)^2\right]\left(1+\frac{s}{41}\right)}$

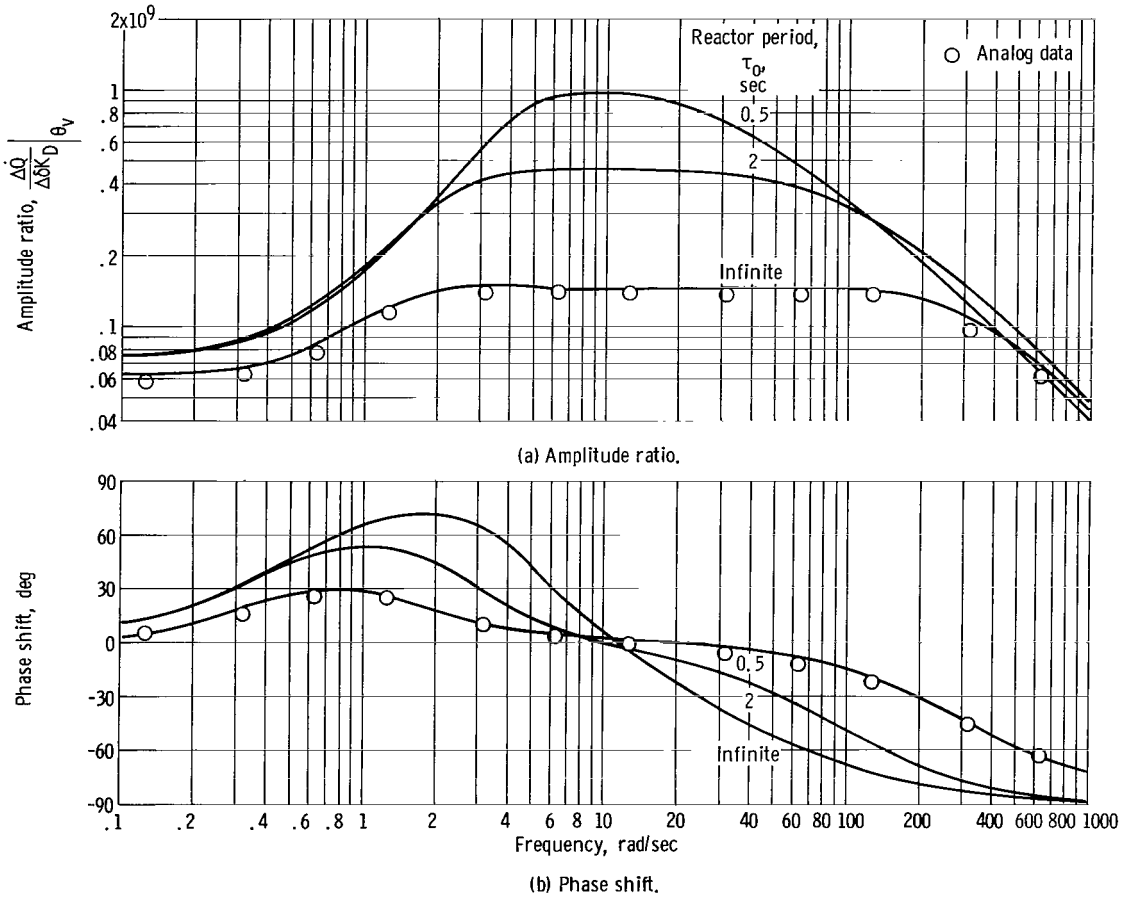

Figure 8. - Frequency response of reactor power to control-drum reactivity at steady-state operating level I for 2 and 0.5 second and infinite reactor periods.

CONCLUDING REMARKS

A nonlinear, wide-range, analog computer simulation was programed from a set of equations that represents the principal dynamics of a nuclear rocket engine system. From this simulation, the following frequency responses and transfer functions, for four selected steady-state operating levels, were obtained: chamber temperature to reactor power, chamber pressure to turbine-control-valve position, and reactor power to control-drum reactivity.

The effect of reactor period on the transfer function of reactor power to control-drum reactivity was investigated. Transfer functions were determined for constant periods of 2.0 and 0.5 second as well as for an infinite period.

The system transfer functions that were developed in this study have been used to perform a controls analysis (ref. 10) and to determine controller transfer functions and closed-loop responses of the system variables.

In reference 10, the control system determined by root-locus analysis was implemented on the analog computer and used to control the system simulation. Closed-loop responses obtained from the analog simulation substantiated the analytically predicted responses.

Lewis Research Center,
National Aeronautics and Space Administration,
Cleveland, Ohio, November 22, 1966,
122-29-03-06-22.

APPENDIX A

SYMBOLS

A	area, ft^2
C_i	concentration of i^{th} group of delayed neutrons (see eq. (7))
c	specific heat, Btu/(lb)(^oR)
c_p	specific heat at constant pressure, Btu/(lb)(^oR)
D	diameter or hydraulic diameter, ft
$F_i()$	function of ( ), where i is an integer
f	friction factor
g	gravitational acceleration, ft/sec^2
H	enthalpy, Btu/lb
h	convective heat-transfer coefficient, Btu/(ft^2)(sec)(^oR)
I	turbopump moment of inertia, (ft)(lb)(sec^2)
J	mechanical heat equivalent, ft-lb/Btu
K_i	constant, where i is an integer
k	thermal conductivity, Btu/(ft)(sec)(^oR)
L	length, ft
ℓ^*	mean effective lifetime of neutrons, sec
M	torque, (ft)(lb)
N	turbopump speed, rpm
n	relative neutron level
P	total pressure, psia
p	static pressure, psia
Pr	Prandtl number, $c_p\mu/k$
$\dot{Q}$	generated thermal power ($\propto$n), Btu/sec
q	heat stored, Btu
R	gas constant for hydrogen, ft/^oR
Re	Reynolds number, $\dot{W}D/A\mu$
s	Laplace transform variable, sec^{-1}
T	temperature, ^oR
t	time, sec
u	velocity, ft/sec
V	volume, ft^3
v	specific volume, ft^3/lb
$\dot{W}$	weight flow rate, lb/sec
Y_i	C_i divided by n
β	total delayed neutrons
β_i	fraction of i^{th} group of delayed neutrons
γ	ratio of specific heats
Δ	change or perturbation
δK	total reactivity
δK_I	inherent reactivity feedback
θ	angular position, deg
λ_i	decay constant of i^{th} group of delayed neutrons, sec^{-1}
μ	absolute viscosity, lb/(ft)(sec)
ρ	density of propellant, lb/ft^3

τ reactor period, sec

Subscripts:

A first reactor-core section

a ambient

B second reactor-core section

b bulk conditions

C third reactor-core section

c reactor-core coolant passages

cb cold bleed

D control drum

d demand

e error

H hydrogen

hb hot bleed

hg hot gas

in inlet

m material

mc reactor-core material

mn nozzle material

mr reflector material

nc nozzle coolant passages

nt nozzle throat

o constant or steady-state value

out outlet

p pump

r reflector coolant passages

s surface

t turbine

ti turbine inlet

te turbine exit

tn turbine nozzle

v turbine control valve

w wall

1 hydrogen tank

2 pump inlet

3 pump outlet

4 nozzle coolant-tube inlet

5 reflector inlet

6 reflector outlet

7 reactor-core inlet

7.1 first core-section outlet

7.2 second core-section outlet

8 reactor outlet chamber

9 bleed mixing volume

10 turbine-control-valve inlet

11 turbine inlet plenum

12 turbine outlet plenum

Superscripts:

$(\bar{})$ average

(') measured variable

APPENDIX B

SYSTEM EQUATIONS

The specific system equations in this appendix are based on design data for a first-generation NERVA-type nuclear rocket engine that develops approximately 56 000 pounds of thrust.

Pump

$$P_2 = P_1 = \text{Const} \tag{B1}$$

$$T_2 = T_1 = \text{Const} \tag{B2}$$

$$\frac{P_3 - P_2}{N^2} = F_1\left(\frac{\dot{W}_p}{N}\right) \tag{B3}$$

$$\frac{M_p}{N^2} = F_2\left(\frac{\dot{W}_p}{N}\right) \tag{B4}$$

$$T_3 = T_2 + 0.14\,\dot{W}_p \tag{B5}$$

$$H_3 = 5.0\,T_3 - 298 \tag{B6}$$

Pump Discharge Line

$$T_4 = T_3 \tag{B7}$$

$$H_4 = H_3 \tag{B8}$$

$$\frac{d\dot{W}_p}{dt} = 31.57\left[P_3 - P_4 - 6.56\times10^{-4}(\dot{W}_p)^2\right] \tag{B9}$$

Nozzle

$$P_4 = P_5 + \dot{W}_p^2 \left(\frac{8.63 \times 10^{-2}}{\rho_4} + \frac{1.81 \times 10^{-2}}{\rho_5} \right) \tag{B10}$$

$$\rho_4 = \text{Const} \tag{B11}$$

$$\rho_5 = 0.1878 \frac{P_5}{T_5} \tag{B12}$$

$$\frac{dq_{mn}}{dt} = 0.32 \, \dot{W}_{nt}^{0.8} (T_8 - \overline{T}_{mn}) - 1.035 \, \dot{W}_{nc}^{0.8} \left(\overline{T}_{mn} - \frac{T_4 + T_5}{2} \right) \tag{B13}$$

$$\overline{T}_{mn} = F_3(q_{mn}) \tag{B14}$$

$$T_5 = 0.294 \left[H_5 + 147 - 1.285 \times 10^{-5} (400 - P_5)(240 - T_5) \right] \tag{B15}$$

$$H_5 = H_4 + 1.035 \, W_p^{-0.2} \left(\overline{T}_{mn} - \frac{T_4 - T_5}{2} \right) \tag{B16}$$

Reflector

$$P_5 = P_6 + \dot{W}_r^2 \left(\frac{1.01 \times 10^{-3}}{\rho_5} + \frac{4.12 \times 10^{-3}}{\rho_6} \right) \tag{B17}$$

$$\dot{W}_r = \dot{W}_p \tag{B18}$$

$$\frac{dq_{mr}}{dt} = K_r \dot{Q} - h_r A_{s,r} \left(\overline{T}_{mr} - \frac{T_5 + T_6}{2} \right) \tag{B19}$$

$$\overline{T}_{mr} = F_4(q_{mr}) \tag{B20}$$

$$T_6 = 2\left[\overline{T}_{mr} - \frac{\dot{W}_r}{h_r A_{s,r}}(H_6 - H_5)\right] - T_5 \tag{B21}$$

$$h_r A_{s,r} = 87.11\,\dot{W}_r^{0.8}(\overline{T}_{mr})^{-0.55} F_5\left(\frac{T_5 + T_6}{2}\right) \tag{B22}$$

$$H_6 = 3.85\,T_6 - 255 \quad \text{for } T_6 \geq 240^{\circ}\,R \tag{B23}$$

$$H_6 = 3.4\,T_6 - 147 + 1.285\times10^{-5}(400 - P_6)(240 - T_6) \quad \text{for } T_6 < 240^{\circ}\,R \tag{B24}$$

Reactor-Core Inlet Plenum

$$\frac{d\rho_6}{dt} = 0.4(\dot{W}_r - \dot{W}_c - \dot{W}_{cb}) \tag{B25}$$

$$P_6 = 5.322\,\rho_6 T_6 \tag{B26}$$

$$P_7 = P_6 \tag{B27}$$

$$T_7 = T_6 \tag{B28}$$

$$H_7 = H_6 \tag{B29}$$

$$\rho_7 = \rho_6 \tag{B30}$$

Reactor-Core Section A

$$\frac{dq_{mc,A}}{dt} = K_A\dot{Q} - h_{c,A}A_{s,c,A}\left(\overline{T}_{mc,A} - \frac{T_7 + T_{7.1}}{2}\right) \tag{B31}$$

$$\overline{T}_{mc,A} = F_6(q_{mc,A}) \tag{B32}$$

$$T_{7.1} = 2\left[\overline{T}_{mc,A} - \frac{\dot{W}_c}{h_{c,1}A_{s,c,A}}(H_{7.1} - H_7)\right] - T_7 \tag{B33}$$

$$h_{c,A}A_{s,c,A} = 72.0\,\dot{W}_c^{0.8}(\overline{T}_{mc,A})^{-0.55}F_7\left(\frac{T_7 + T_{7.1}}{2}\right) \tag{B34}$$

$$H_{7.1} = 3.51\,T_{7.1} - 90 \tag{B35}$$

Reactor-Core Section B

$$\frac{dq_{mc,B}}{dt} = K_B\dot{Q} - h_{c,B}A_{s,c,B}\left(\overline{T}_{mc,B} - \frac{T_{7.1} + T_{7.2}}{2}\right) \tag{B36}$$

$$\overline{T}_{mc,B} = F_6(q_{mc,B}) \tag{B37}$$

$$T_{7.2} = 2\left[\overline{T}_{mc,B} - \frac{\dot{W}_c}{h_{c,B}A_{s,c,B}}(H_{7.2} - H_{7.1})\right] - T_{7.1} \tag{B38}$$

$$h_{s,B}A_{s,c,B} = 72.0\,\dot{W}_c^{0.8}(\overline{T}_{mc,B})^{-0.55}F_7\left(\frac{T_{7.1} + T_{7.2}}{2}\right) \tag{B39}$$

$$H_{7.2} = 3.51\,T_{7.2} - 90 \quad \text{for } T_{7.2} \leq 2000^{\circ}\,R \tag{B40}$$

$$H_{7.2} = 3.77\,T_{7.2} - 610 \quad \text{for } 2000^{\circ}\,R \leq T_{7.2} \leq 3000^{\circ}\,R \tag{B41}$$

$$H_{7.2} = 4.09\,T_{7.2} - 1570 \quad \text{for } T_{7.2} \geq 3000^{\circ}\,R \tag{B42}$$

Reactor-Core Section C

$$\frac{dq_{mc,C}}{dt} = K_C\dot{Q} - h_{c,C}A_{s,c,C}\left(\overline{T}_{mc,C} - \frac{T_{7.2} + T_8}{2}\right) \tag{B43}$$

$$\overline{T}_{mc,C} = F_6(q_{mc,C}) \tag{B44}$$

$$T_8 = 2\left[\overline{T}_{mc,C} - \frac{\dot{W}_c}{h_{c,C}A_{s,c,C}}(H_8 - H_{7.2})\right] - T_{7.2} \tag{B45}$$

$$h_{c,C}A_{s,c,C} = 72.0\,\dot{W}_c^{0.8}(\overline{T}_{mc,C})^{-0.55}F_7\left(\frac{T_{7.2} + T_8}{2}\right) \tag{B46}$$

$$H_8 = 3.51\,T_8 - 90 \quad \text{for} \quad T_8 \leq 2000^{\circ}\,R \tag{B47}$$

$$H_8 = 3.77\,T_8 - 610 \quad \text{for} \quad 2000^{\circ}\,R \leq T_8 \leq 3000^{\circ}\,R \tag{B48}$$

$$H_8 = 4.09\,T_8 - 1570 \quad \text{for} \quad T_8 \geq 3000^{\circ}\,R \tag{B49}$$

Reactor-Core Weight Flow

$$\dot{W}_c = \left(\frac{P_7 - P_8}{4.475\times10^{-3}v_7 + 3.807\times10^{-4}v_8}\right)^{0.5} \tag{B50}$$

$$v_7 = \frac{1}{\rho_7} \tag{B51}$$

$$v_8 = \frac{1}{\rho_8} \tag{B52}$$

Thrust Chamber and Nozzle

$$\frac{d\rho_8}{dt} = 0.1(\dot{W}_c - \dot{W}_{nt} - \dot{W}_{hb}) \tag{B53}$$

$$P_8 = 5.322\,\rho_8 T_8 \tag{B54}$$

$$\dot{W}_{nt} = 8.139 \frac{P_8}{T_8^{0.5}} \tag{B55}$$

Reactor Kinetics

$$\frac{dn}{dt} = (40\,000\delta K - 312.0)n + \sum_{i=1}^{6} \lambda_i C_i \tag{B56}$$

$$\frac{dC_1}{dt} = 11.856\ n - 0.0127\ C_1 \tag{B57}$$

$$\frac{dC_2}{dt} = 66.456\ n - 0.0317\ C_2 \tag{B58}$$

$$\frac{dC_3}{dt} = 58.656\ n - 0.115\ C_3 \tag{B59}$$

$$\frac{dC_4}{dt} = 126.984\ n - 0.311\ C_4 \tag{B60}$$

$$\frac{dC_5}{dt} = 39.936\ n - 1.40\ C_5 \tag{B61}$$

$$\frac{dC_6}{dt} = 8.112\ n - 3.87\ C_6 \tag{B62}$$

Reactivity Summation

$$\delta K = \delta K_D + \delta K_o \tag{B63}$$

$$\delta K_I = F_8(\overline{T}_{mc}, \overline{\rho}_{H,c}) \tag{B64}$$

$$\bar{\rho}_{H,c} = 0.1878 \frac{P_7}{T_8 - T_7} \ln \frac{T_8}{T_7} \tag{B65}$$

$$\bar{T}_{mc} = \frac{T_{mc,A} + T_{mc,B} + T_{mc,C}}{3} \tag{B66}$$

Bleed System

$$\frac{d\rho_9}{dt} = 1.0(\dot{W}_{cb} + \dot{W}_{hb} - \dot{W}_v) \tag{B67}$$

$$P_9 = 5.322\, \rho_9 T_9 \tag{B68}$$

$$\frac{dH_9}{dt} = \frac{\dot{W}_{hb} H_8}{\rho_9} + \frac{\dot{W}_{cb} H_6}{\rho_9} - \frac{\dot{W}_v H_9}{\rho_9} \tag{B69}$$

$$T_9 = \frac{H_9 + 90}{3.51} \tag{B70}$$

$$\dot{W}_{cb} = 0.542 \frac{A_{cb} P_6}{T_6^{0.5}} F_9\left(\frac{P_9}{P_6}\right) \tag{B71}$$

$$\dot{W}_{hb} = 0.542 \frac{A_{hb} P_8}{T_8^{0.5}} F_9\left(\frac{P_9}{P_8}\right) \tag{B72}$$

$$\dot{W}_v = 0.542 \frac{A_v P_{10}}{T_{10}^{0.5}} F_9\left(\frac{P_{11}}{P_{10}}\right) \tag{B73}$$

$$A_v = F_{10}(\theta_v) \tag{B74}$$

$$P_{10} = P_9 \tag{B75}$$

$$T_{10} = T_9 \tag{B76}$$

Turbine

$$\frac{d\rho_{11}}{dt} = 1.0(\dot{W}_v - \dot{W}_{ti}) \tag{B77}$$

$$P_{11} = 5.322\ \rho_{11} T_{11} \tag{B78}$$

$$T_{11} = T_{10} \tag{B79}$$

$$\dot{W}_{ti} = \frac{P_{11}}{T_{11}^{0.5}} F_{11}\left(\frac{P_{12}}{P_{11}}\right) \tag{B80}$$

$$M_t = \dot{W}_{ti}\left\{12.61\ T_{11}^{0.5}\left[1 - \left(\frac{p_{12}}{P_{11}}\right)^{0.286}\right]^{0.5} - 2.85\times10^{-3} N\right\} \tag{B81}$$

$$T_{12} = T_{11} - 3.835\times10^{-5}\frac{M_t N}{\dot{W}_{ti}} \tag{B82}$$

$$\frac{d\rho_{12}}{dt} = 1.0(\dot{W}_{ti} - \dot{W}_{tn}) \tag{B83}$$

$$P_{12} = 5.322\ \rho_{12} T_{12} \tag{B84}$$

$$p_{12} = P_{12} - 1.324\times10^{-2}\frac{\dot{W}_{ti}^2}{\rho_{12}} \tag{B85}$$

$$\dot{W}_{tn} = 0.542\frac{A_{tn} P_{12}}{T_{12}^{0.5}} F_9\left(\frac{P_a}{P_{12}}\right) \tag{B86}$$

Torque Balance

$$\frac{dN}{dt} = 79.0(M_t - M_p) \tag{B87}$$

APPENDIX C

REACTOR-KINETICS TRANSFER FUNCTION

The reactor-kinetics equations can be written in logarithmic form:

$$\frac{d}{dt}(\ln n) = \frac{\delta K - \beta}{l^*} + \sum_i \lambda_i Y_i \tag{C1}$$

$$\frac{dY_i}{dt} = \frac{\beta_i}{l^*} - \lambda_i Y_i - Y_i \frac{d}{dt}(\ln n) \tag{C2}$$

The following transfer function can be derived (ref. 8) from these equations by using a perturbation analysis.

$$\frac{\Delta \ln n(s)}{\Delta \delta K(s)} = \frac{1}{l^* s \left[1 + \sum_i \frac{\beta_i}{l^*(s + \lambda_i)}\right]} \tag{C3}$$

In the perturbation analysis that led to this transfer function, it was assumed that the steady-state power level n_o was constant and that the steady-state reactivity δK_o was zero.

Reference 8 shows that another reactor transfer function can be derived by assuming that the reactor power level is rising exponentially and that the reactivity is constant. This transfer function is

$$\frac{\Delta \ln n(s)}{\Delta \delta K(s)} = \frac{1}{l^* s \left[1 + \sum_i \frac{\beta_i}{l^*} \frac{\lambda_i}{\left(\lambda_i + \frac{1}{\tau_o}\right)} \frac{1}{\left(s + \lambda_i + \frac{1}{\tau_o}\right)}\right]} \tag{C4}$$

In reference 9, the following values of β_i/β and λ_i for a three-delay-group approximation of the reactor-kinetic parameters are given:

$$\frac{\beta_1}{\beta} = 0.274 \qquad \lambda_1 = 0.0276$$

$$\frac{\beta_2}{\beta} = 0.559 \qquad \lambda_2 = 0.235$$

$$\frac{\beta_3}{\beta} = 0.167 \qquad \lambda_3 = 1.65$$

By using these values, $\ell^* = 25\times10^{-6}$ second, and $\beta = 0.0078$, the following transfer functions were calculated for constant periods of infinity, 2 seconds, and 0.5 second.

For $\tau_o = \infty$,

$$\frac{\Delta \ln n(s)}{\Delta\delta K(s)} = \frac{10.32\left(1+\frac{s}{0.0276}\right)\left(1+\frac{s}{0.235}\right)\left(1+\frac{s}{1.65}\right)}{s\left(1+\frac{s}{0.095}\right)\left(1+\frac{s}{1.398}\right)\left(1+\frac{s}{312.42}\right)} \tag{C5}$$

For $\tau_o = 2$ seconds,

$$\frac{\Delta \ln n(s)}{\Delta\delta K(s)} = \frac{3.848\times10^{2}\left(1+\frac{s}{0.528}\right)\left(1+\frac{s}{0.735}\right)\left(1+\frac{s}{2.15}\right)}{s\left(1+\frac{s}{0.541}\right)\left(1+\frac{s}{1.578}\right)\left(1+\frac{s}{101.52}\right)} \tag{C6}$$

For $\tau_o = 0.5$ second,

$$\frac{\Delta \ln n(s)}{\Delta\delta K(s)} = \frac{2.465\times10^{3}\left(1+\frac{s}{2.028}\right)\left(1+\frac{s}{2.235}\right)\left(1+\frac{s}{3.65}\right)}{s\left(1+\frac{s}{2.04}\right)\left(1+\frac{s}{2.86}\right)\left(1+\frac{s}{46.1}\right)} \tag{C7}$$

The equivalent linear form of these transfer functions (i.e., $\Delta\dot{Q}(s)/\Delta\delta K(s)$, with power expressed as thermal power) can be obtained by multiplying the logarithmic form by $\dot{Q}_o$, which is the steady-state power level.

REFERENCES

1. Wasserman, A. A.; Bodenschatz, C. A.; Steiner, G. H.; James, L. R.; Balcomb, J. D.; Johnson, J. A.; and Springer, T. E.: Review of Transfer Function Measurements in The Nuclear Rocket Program Using Noise Techniques. Paper No. 66-682, AIAA, June 1966.

2. Felix, Bernard, R.; and Bohl, Richard J.: Dynamic Analysis of a Nuclear Rocket Engine System. ARS J., vol. 29, no. 11, Nov. 1959, pp. 853-862.

3. Mohler, Ronald R.: Stability and Control of Nuclear Rocket Propulsion. Paper Presented at the Joint Automatic Control Conference, IRE, Cambridge, Mass., Sept. 7-9, 1960.

4. Thomas, G. R.: An Interim Study of Single Phase Heat Transfer Correlations Using Hydrogen. Rep. No. WANL-TNR-056, Astronuclear Lab., Westinghouse Electric Corp., Apr. 1962.

5. Keepin, G. R.; and Wimett, T. F.: Reactor Kinetic Functions -- A New Evaluation. Nucleonics, vol. 16, no. 10, Oct. 1958, pp. 86-90.

6. Morgan, M. L.; and Looney, J. C.: Design of the ESIAC Algebraic Computer. IRE Trans. on Electronic Computers, vol. EC-10, no. 3, Sept. 1961, pp. 524-529.

7. Morgan, M. L.: The Construction and Use of Logarithmic Pole-Zero, Root Locus and Frequency Response Plots. Preprint No. 2.2.63, ISA, Sept. 1963.

8. Singer, Sidney: The Period Equilibrium Effect in Reactor Dynamics. Rep. No. LA-2654, Los Alamos Scientific Laboratory, Jan. 1962.

9. Hearn, Thomas O.: NRDS Analysis of the KIWI B-4D-202 Nuclear Reactor Control System. Rep. No. LA-3301-MS, Los Alamos Scientific Laboratory, Aug. 1964.

10. Arpasi, Dale J.; and Hart, Clint E.: Controls Analysis of Nuclear Rocket Engine at Power Range Operating Conditions. NASA TN D-3978, 1967.

NASA-Langley, 1967 —— 22 E-3665

"The aeronautical and space activities of the United States shall be conducted so as to contribute . . . to the expansion of human knowledge of phenomena in the atmosphere and space. The Administration shall provide for the widest practicable and appropriate dissemination of information concerning its activities and the results thereof."

—NATIONAL AERONAUTICS AND SPACE ACT OF 1958

NASA SCIENTIFIC AND TECHNICAL PUBLICATIONS

TECHNICAL REPORTS: Scientific and technical information considered important, complete, and a lasting contribution to existing knowledge.

TECHNICAL NOTES: Information less broad in scope but nevertheless of importance as a contribution to existing knowledge.

TECHNICAL MEMORANDUMS: Information receiving limited distribution because of preliminary data, security classification, or other reasons.

CONTRACTOR REPORTS: Scientific and technical information generated under a NASA contract or grant and considered an important contribution to existing knowledge.

TECHNICAL TRANSLATIONS: Information published in a foreign language considered to merit NASA distribution in English.

SPECIAL PUBLICATIONS: Information derived from or of value to NASA activities. Publications include conference proceedings, monographs, data compilations, handbooks, sourcebooks, and special bibliographies.

TECHNOLOGY UTILIZATION PUBLICATIONS: Information on technology used by NASA that may be of particular interest in commercial and other non-aerospace applications. Publications include Tech Briefs, Technology Utilization Reports and Notes, and Technology Surveys.

Details on the availability of these publications may be obtained from:

SCIENTIFIC AND TECHNICAL INFORMATION DIVISION

NATIONAL AERONAUTICS AND SPACE ADMINISTRATION

Washington, D.C. 20546